Available online at www.sciencedirect.com
SCIENCE DIRECT®
Journal of Photochemistry and Photobiology A: Chemistry 159 (2003) 89–99
Journal of Photochemistry and Photobiology A:Chemistry
www.elsevier.com/locate/jphotochem

An innovative coupled solar-biological system at field pilot scale for the treatment of biorecalcitrant pollutants

Victor Sarria [a], Siméon Kenfack [a], Olivier Guillod [b], César Pulgarin [a,*]

[a] *Laboratory for Environmental Biotechnology, Institute of Environmental Science and Technology, Swiss Federal Institute of Technology (EPFL), CH-1015 Lausanne, Switzerland*
[b] *DLK Technologies SA, Jambe-Ducommun 6a, CH-2400 Le Locle, Switzerland*

Received 13 February 2003; received in revised form 13 February 2003; accepted 3 March 2003

Abstract

An overview of recent works (1998–2002) coupling Advanced Oxidation Process (AOP) and Biological systems for wastewater treatment confirms the beneficial effects of such two-steps treatment at lab scale. In this paper, an innovative coupled solar-biological system at field pilot scale was designed, builds, and experimental results are presented. The strategy to develop this system implicates the choice of the most appropriate solar collector and the most efficient AOP, the optimization of this AOP, the choice of the biological oxidation system, the monitoring of the chemical and biological characteristics of photo-treated solutions and the evaluation of the performances of the coupled solar-biological flow system. The coupled system is conformed by a Compound Parabolic Solar Collector (CPC) and a Fixed Bed Reactor (FBR). The photo-Fenton system was the most appropriate AOP for the degradation of a model biorecalcitrant compound, 5-amino-6-methyl-2-benzimidazolone (AMBI). Surface Response Methodology was used to optimize the Fe^{3+} and H_2O_2 concentration. The coupled reactor, operates in semicontinuous mode, has shown to reach a whole mineralization performance between 80 and 90% in the range of initial dissolved organic carbon (DOC) concentration of 300–500 mg C l^{-1}. These results indicate that coupling solar-biological processes at pilot scale is a plausible effective approach for the treatment of real industrial wastewaters.

Keywords: AOP; Coupled oxidation systems; Fixed Bed Reactor; Photo-Fenton; Pilot scale reactor; Solar photocatalysis; Wastewater treatment

1. Introduction

Advanced Oxidation Processes (AOPs) are very promising methods for the remediation of contaminated wastewaters containing non-biodegradable organic pollutants [1]. Nevertheless, one of the major drawbacks of these AOPs is that their operational costs are relatively high compared to those of biological treatments. However, the use of AOPs as a pretreatment step to enhance the biodegradability of wastewater containing recalcitrant or inhibitory compounds can be justified if the resulting intermediates are easily degradable in a further biological treatment.

Previous studies have attempted the strategy of combining chemical and biological processes to treat contaminants in wastewater. These studies, extensively reviewed by Scott and Ollis [2,3] suggested potential advantages for water treatment.

Recently, some interesting coupled systems (photoassisted AOP-biological) have been proposed to treat various types of industrial wastewaters. In this paper, most of these former works realized within the last 5 years and based on the structure proposed by Scoot and Ollis [2], were reviewed (Table 1).

Wastewaters under study are coming from: textile, pulp and paper, surfactants, and explosive military industries, as well as from olives washing, and pesticides contaminated effluents.

For the 16 cases shown in Table 1, 2 cases were previously biologically pretreated to remove the easily biodegradable fraction of pollution before leading to the classical schema AOP-biological treatment in which the main aim of the AOP is to produce biodegradable intermediate, or partial mineralisation.

The proposed systems include: $h\nu/H_2O_2$—aerobic batch activated sludge (BAS) [4]. TiO_2-assisted photocatalytic reduction in series with fungal mineralization by phanerochaete chrysosporium [6]. $h\nu/TiO_2$-supported in glass rings followed by bacterial degradation using *Pseudomonas paucimobilis* (S37) and *Burkholdeira cepacia* (PZK) [14]. Ledakowicz et al. [7] explored $h\nu/O_3$ and $h\nu/H_2O_2$ systems as a pretreatment followed by activated sludge. Benitez et al.

* Corresponding author. Tel.: +41-21-693-4720; fax: +41-21-693-4722.
E-mail address: cesar.pulgarin@epfl.ch (C. Pulgarin).

1010-6030/03/$ – see front matter © 2003 Elsevier Science B.V. All rights reserved.
doi:10.1016/S1010-6030(03)00105-9

Table 1
Studies utilizing photochemical (UV) and biological degradation of organic compounds

Authors	Chemical degraded	Concentration	Photoassisted AOPs	Biological oxidation method	Biodegradability test	Order of schema	Grade
Adams and Kuzhikannil [4]	Alkildimethzlbenzyl-ammonium-chlorides Dioctyl-dimethyl-ammonium-chloride	COD = 1000 mg l^{-1}	$h\nu/H_2O_2$	BAS essay	BAS essay	AOP-B	++ 0
Benitez et al. [5]	Olives washing wastewaters	COD = 2.7 g l^{-1}, BOD = 1.56 g l^{-1}	$h\nu/O_3$	Acclimated activated sludge culture	Kinetic measurements (Contois model)	B-AOP AOP-B	+ ++
Hess et al. [6]	TNT	0.44 mmol l^{-1}	$h\nu/TiO_2$	Fungal mineralization by phanerochaete chrysosporidium			++
Ledakowicz et al. [7]	Synthetic textile wastewater	COD = 2154 mg O_2 l^{-1}, BOD = 1050 mg O_2 l^{-1}, PTC = 442 mg C l^{-1}	$h\nu/O_3$, $h\nu/H_2O_2$	Acclimated activated sludge culture	Kinetic measurements (Monod model)	AOP-B	++
Parra et al. [8]	Isoproturon Metobromuron	0.2 mmol l^{-1}	$h\nu/Fe^{3+}/H_2O_2$	FBR	BOD_5/COD Microtox	AOP-B	++ 0
Parra et al. [15]	Isoproturon	0.2 mmol l^{-1}	$h\nu/TiO_2$ immobilized	FBR	BOD_5/COD Microtox	AOP-B	++
Pulgarin et al. [9]	*p*-Nitro-*o*-toluenesulfonic acid	330 mg C l^{-1}	$h\nu/Fe^{3+}/H_2O_2$	FBR	BOD_5/COD Microtox	AOP-B	++
Rodriguez et al. [10]	Textile wastewater	900 mg C l^{-1}	$h\nu/Fe^{3+}/H_2O_2$	FBR	Zhan–Wellens test	AOP-B	0
Reyes et al. [11]	Kraft effluents		$h\nu$/ZnO immobilized	Fungal mineralization by Lentinula edodes		B-B-AOP AOP-B	+ ++
Sarria et al. [12]	AMBI	3 mmol l^{-1}	$h\nu/Fe^{3+}/H_2O_2$	FBR	BOD_5/COD AOS	AOP-B	++
Sarria et al. [13]	AMBI	1 mmol l^{-1}	$h\nu/Fe^{3+}/O_2$	FBR	AOS	AOP-B	++
Yeber et al. [14]	6-Chloro vanillin	186 ppm	$h\nu/TiO_2$ immobilized	*Pseudomonas paucimobilis* (S37), *Burkholdeira cepacia* (PZK)	Bacterial growth rate	AOP-B	++

[5] compared a variety of oxidation schemes: aerobic biological pretreatment followed by either $h\nu/O_3$ or $h\nu/H_2O_2$, and $h\nu/O_3$ or $h\nu/H_2O_2$ pretreatments followed by aerobic biodegradation. Reyes et al. [11] tested a photo-pretreatment using ZnO immobilized on sand followed by a fungal mineralization by Lentinula edodes. Three different combined systems were developed at the EPFL, using photo-Fenton reaction [8–10,12], $h\nu/Fe^{3+}/O_2$ [13] or $h\nu/TiO_2$-supported in glass rings [15]. In all cases this was followed by a biological step with an immobilized biomass system. All these processes are carried in sequential batch reactors at laboratory scale treating 1–3 l of polluted water.

1.1. Photoassisted AOPs system

The four commonly used photoassisted AOPs are: (i) the photodecomposition of hydrogen peroxide ($h\nu/H_2O_2$) [4], (ii) photolysis of ozone ($h\nu/O_3$) [5], (iii) heterogeneous photocatalysis ($h\nu/TiO_2$) [6], and (iv) $h\nu$/ZnO [11]. More improving works are now concentrated on fixing the catalyst on a support, so to work at neutral pH and reuse the catalyst several times [15].

Among AOPs, the photo-Fenton system ($h\nu/Fe^{3+}/H_2O_2$) has shown to be the most promising for remediation of contaminated waters [9]. This process is theoretically stated by the following equations [16]:

$$Fe^{3+} + H_2O + h\nu \rightarrow {}^{\bullet}OH + H^+ + Fe^{2+} \quad (1)$$

$$Fe^{2+} + H_2O_2 \rightarrow {}^{\bullet}OH + {}^{-}OH + Fe^{3+} \quad (2)$$

$$Fe^{3+} + H_2O_2 \rightarrow Fe^{2+} + H^+ + {}^{\bullet}O_2H \quad (3)$$

$$Fe^{2+} + {}^{\bullet}OH \rightarrow Fe^{3+} + {}^{-}OH \quad (4)$$

$$Fe^{2+} + {}^{\bullet}O_2H \rightarrow Fe^{3+} + {}^{-}O_2H \quad (5)$$

$${}^{\bullet}OH + RH \rightarrow R^+ \text{ or } [HORH]^{\bullet} \quad (6)$$

The $h\nu/Fe^{3+}/O_2$ has previously been proposed [17] as an alternative to the use of photo-Fenton ($h\nu/Fe^{3+}/H_2O_2$) since addition of H_2O_2 is avoide

1.2. Biological oxidation system

The choice of the biological oxidation system is a very important point for the development of a coupled system. Same as the choice of AOP, the appropriated biological system depends on the characteristics of the wastewater to be treated, and specifically on the goal of the treatment.

Immobilized-cell aerobic technology which involves the colonization of micro-organisms onto inorganic supports forming a biofilm, has been used for the biodegradation of different types of wastewaters [18]. The immobilized-cell bioreactor or Fixed Bed Reactor (FBR) offers several advantages over conventional suspended growth systems, such as the capacity to handle shock loads [19]. Moreover, it is more resistant to antimicrobial agents, allows the recycling of the biological catalysers, and functions at very high cell concentration without rheological or mass transfer limitations. FBR operating in continuous mode do not suffer of decrease in the metabolic activity due to product accumulation; the use of substrates is optimal even at low concentration. Due to the localized concentration of nutrients and hydrolytic coenzymes at the support-substrate/interface, cells are used in their stationary phase where the metabolic chains are more active.

Other biological process, i.e. the fungal biotreatment has been successfully used to mineralize photo-pretreated solutions of 2,6,6-trinitroleluene (TNT) [6] and 6-chlorovanillin [11].

1.3. Biodegradability test

The biodegradability of the AOP pretreated solutions of initial biorecalcitrant wastewaters is followed or assessed by means of: (i) analyzing global parameters, such as biological oxygen demand (BOD_5), chemical oxygen demand (COD), dissolved organic carbon (DOC), and oxygen uptake (respirometric methods); (ii) estimating the ratio BOD_5/COD or the average oxidation state (AOS); (iii) measuring the bacterial growth rate; (iv) assessing toxicity by measuring the EC_{50} value by Microtox test; or (v) using kinetic models, which according to Ollis [20], is a crucial way to impulse the practical application and design of these coupled systems.

Ledakowicz et al. [7] used the Monod model, which describes the effect of nutrient concentration S on the microbial growth (dX/dt) rate.

$$\frac{dX}{dt} = \frac{\mu_{max} S}{K_m + S} X \quad (7)$$

here, μ_{max} is the maximum specific growth rate, and K_m is the saturation constant for substrate (Monod constant).

Benitez et al. [5] employed the Contois model, which relates the specific substrate decomposition rate q to the substrate concentration S.

$$q = \frac{q_{max} S}{K_1 X + S} \quad (8)$$

In Eq. (8) q_{max} is the maximum rate of substrate utilization and K_1 is the Contois saturation constant.

1.4. Overall processes efficiency

The final column of Table 1 (Grade) presents indicators of overall effectiveness for combined oxidation studies. The following convention were used: (++) for a dramatic increase, (+) for a modest increase, and (0) for a negligible increase. Coupled systems generally lead to increase the degradation of target compounds. Among the 16 cases of Table 1, dramatic increase (++) was noted in 11 cases, modest increase (+) in 2 cases, and a negligible increase (0) in 3 cases. The negative results were attributed to the formation of uncharacterized biorecalcitrant intermediates and complexes [4,8,10].

For all the studies leading to Table 1 results, only Yeber et al. [14] realized a GC/MS analysis in order to determine the structure of some oxidation by-products and proposed a pathway for the photocatalytic degradation of 6-cholovanillin.

In general, works summarized in Table 1, confirm the convenience of sequential photochemical and biological oxidation of biorecalcitrant pollutants. Nevertheless, to date do not exist study that explore the possible combination of solar and biological processes at pilot scale.

This work aimed to design, build and operate on the first coupled solar-biological system at pilot scale to follow the treatment of biorecalcitrant pollutants in wastewaters. 5-Amino-6-methyl-2-benzimidazolone (AMBI), a dye precursor widely used in chemical industry was chosen as model pollutant since previous works on photocatalytic degradation of this chemical are known [13].

Photo-Fenton system was used in the pretreatment, since this method has shown to be the most effective among different tested AOPs and the following biodegradation process was carried in an Immobilized Activated Sludge bioreactor.

In this paper, the following topics are also studied: (a) the choice of the most appropriate solar collector. This part of the study was carried at the Plataforma Solar de Almeria (PSA). (b) The optimization of Fe^{3+} and H_2O_2 concentrations in the photo-degradation process using Response Surface Methodology (RSM). (c) The biodegradability of the photo-treated solutions. (d) The performance of the coupled solar-biological flow system.

2. Experimental

2.1. Reagents

All chemicals were used as received without further purification. AMBI ($C_8H_9N_3O$) as well as samples of real industrial wastewater were received from Rohner, Basel, Switzerland. $FeCl_3{\cdot}6H_2O$ and H_2O_2 (30% w/w) analysis grade (p.a.) were from Fluka, and TiO_2 was Degussa P-25, mainly anatase with a surface area of $50\,m^2\,g^{-1}$. The chemicals for HPLC analysis were obtained from Fluka. Milli-Q water was used throughout for the preparation of aqueous solutions and as a component of the mobile phase, water–acetonitrile (HPLC grade) in HPLC analysis. The photo-treated solutions were neutralized by means of NaOH. Neutral pH of the solutions was maintained during the biological treatment by adjusting with HCl or NaOH.

2.2. Coupled solar-biological system at pilot scale

The investigation was carried out using a coupled solar-biological solar reactor that has been designed, built and operated at the EPFL. This system is conformed by a Compound Parabolic Solar Collector (CPC) and a bioreactor as illustrated in Fig. 1.

2.2.1. Solar reactor

The configuration of the CPC is the same as that at the PSA [21]. CPC is a static collector with a reflective surface describing an in-volute around a cylindrical reactor tube. Due to the reflector design shown in Fig. 2b, almost all the UV radiation arriving at the CPC aperture area (not only direct, but also diffuse) can be collected and so be available for the process in the reactor. The UV light reflected by the CPC is distributed around the back of the tubular photoreactor and as a result, most of the reactor tube circumference is illuminated.

The CPC has three modules (collector surface $3.08\,m^2$, photoreactor volume 24 l, and total reactor volume 60 l) whereas one module consists of eight tubes and mounted on a fixed platform 46° tilted (local latitude). The three modules are connected in series with water directly flowing through them at $30\,l\,min^{-1}$, leading finally to a recirculation tank connected to a centrifugal pump.

Solar ultraviolet radiation is determined during the experiments by means of a global UV radiometer (KIPP&ZONEN, model CUV3) shown in Fig. 2c, also mounted on a 46° fixed-angle platform (the same angle as the CPC). It provides data in terms of global UV solar energy power incident per unit area, $W_{UV}\ m^{-2}$. Solar-UV power varies during experiments, especially when clouds are passing by. Data combination from several days and their comparison with other photocatalytic experiments is done by the application of Eq. (9).

$$Q_{UV,n} = Q_{UV,n-1} + \Delta t_n\,\overline{UV}_{G,n}\,\frac{A_{CPC}}{V_{TOT}} \tag{9}$$

where $\Delta t_n = t_n - t_{n-1}$, t_n is the experimental time for each sample, $\overline{UV}_{G,n}$ is the average UV_G (global UV radiation) during Δt_n, $A_{CPC} = 3.08\,m^2$, $V_{TOT} = 39\,l$, and $Q_{UV,n}$ is the accumulated energy incident on the photoreactor for each sample during the experiment per unit of volume ($kJ\,l^{-1}$).

2.2.2. Biological reactor

The bioreactor is conformed by three modules: a 50-l conditioning container, a FBR, and a decanter. The conditioning container is equipped with a pH control unit (Liquisys, Endress + Hauser) for pH adjustment using either HCl or NaOH. A 1-l tank was installed to supply nutrients (N, P, K, and microelements) that may be used. The photo-pretreated water is piped across the bottom layer to the FBR by means of a centrifugal pump. The FBR consist of a 43-l column containing plastic supports (Material: Polypropylene; nominal diameter: 15 mm, density: $80\,kg\,m^{-3}$, voluminal surface: $320\,m^2\,m^{-3}$, empty space fraction: $0.91\,m^3\,m^{-3}$) colonized by activated sludge from the municipal wastewater treatment plant of Vidy, Lausanne, Switzerland. The effluent is circulated through the column which operates as an up-flow reactor. The FBR is equipped with an air blower to supply oxygen ($1.15\,m^3\,min^{-1}$ of air) to the micro-organisms. The recirculation flow rate is $10\,l\,min^{-1}$. The top treated water over-flows to a 50-l decanter, where sludge is extracted. The

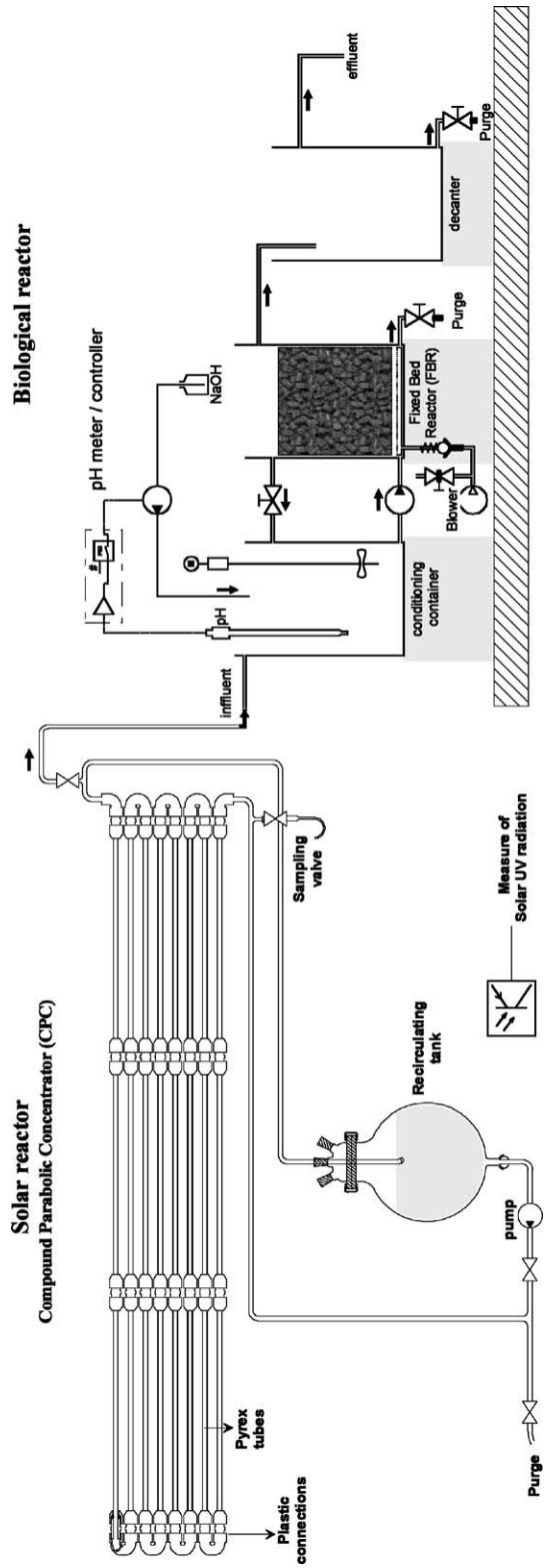

Fig. 1. Schematic representation of the coupled solar-biological flow reactor.

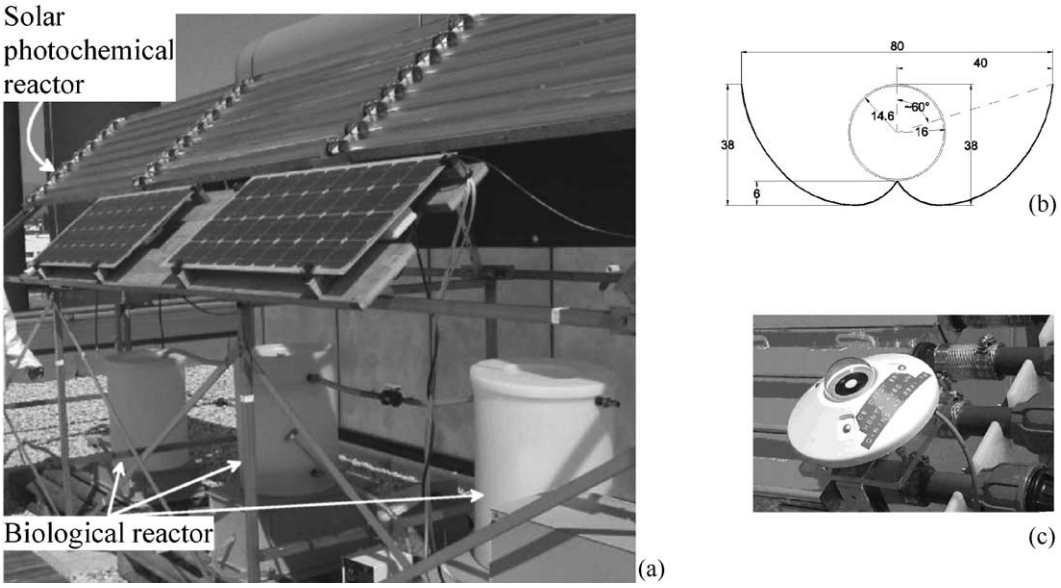

Fig. 2. (a) The pilot coupled solar-biological flow reactor at EPFL, (b) reflective surface describing an in-volute around a cylindrical tube on the CPC, and (c) view of the solar UV radiometer.

schematic diagram of the pilot system is shown in the right hand side of Fig. 1.

2.3. Parabolic-trough concentrator

The parabolic-trough concentrator (PTC), previously described in detail [22], consists of a turret with a platform supporting four parabolic-trough collectors (PTCs) with focus-absorber tubes. The platform is moved by two motors controlled by a two-axis (azimuth and elevation) tracking system. The tracking system consists of a photochemical cell keeping the aperture plane perpendicular to the solar rays, which are reflected onto the focus (absorber) through which circulates water to be treated.

During the experiments performed using the PTC at the PSA, the direct UV radiation has been determined using a direct-UV sensor (International Light-ESD 400), which is mounted on the sun-tracking platform. With Eq. (9) the accumulated energy per unit of volume incident on the reactor (Q_{UV}) has been calculated, taking into account the PCT dimensions: $A_{PTC} = 29\,m^2$ and $V_{TOT} = 260\,l$.

2.4. Chemical analysis

DOC measurements were performed using a TOC analyzer (Shimadzu, Model 5050A) equipped with an ASI automatic sample injector. It uses a potassium phthalate solution as calibration standard. COD was carried out via a Hach-2000 spectrophotometer using dichromate solution as oxidant in strong acid media. High performance liquid chromatography (HPLC) was carried out in a Varian 9065 unit provided with a Varian 9012 solvent delivery system, an automatic injector 9100, and a Varian Pro Star Variable (200–400) diode array detector 9065 Polychrom. All modules are piloted with a PC computer with the Varian Star 5.3 software for liquid chromatography. A reverse phase Spherisorb silica column ODS-2 and ammonium acetate/acetonitrile as mobile phase are used to run the chromatography in gradient mode.

3. Results

3.1. Choice of the solar photoreactor: comparison between medium and low concentrating solar collectors during the iron-photoassisted degradation of AMBI

This part of the study, carried out at the PSA, focuses on the comparison of performance of two types of solar collectors in order to find out the more suitable to be used in a pilot coupled solar-biological flow system. A medium concentrating system, two-axis PTC, and a low concentrating system CPC were compared. The $h\nu/Fe^{3+}/O_2$ photocatalytic system was chosen, considering that its performance is only related to the radiation absorbed by the solar reactors. This system was successfully tested for the degradation of AMBI [13].

Fig. 3 shows the linear relation between $-\ln(C/Co)$ and Q_{UV} for the AMBI disappearance in the reactors. In both cases, the kinetic of AMBI degradation is apparent first order, and its performances are quit similar, with a rate constant (k_{app}) equal to 0.0121 and $0.0112\,l\,kJ^{-1}$ for the CPC and the PTC Reactors respectively. In order to explain this result and to choose the best technology, more other factors were taken into account:

- The ability of the CPC to capture both diffuse and direct UV radiation. In contrast, a concentrating design like that of the PTC benefits only the direct UV radiation.

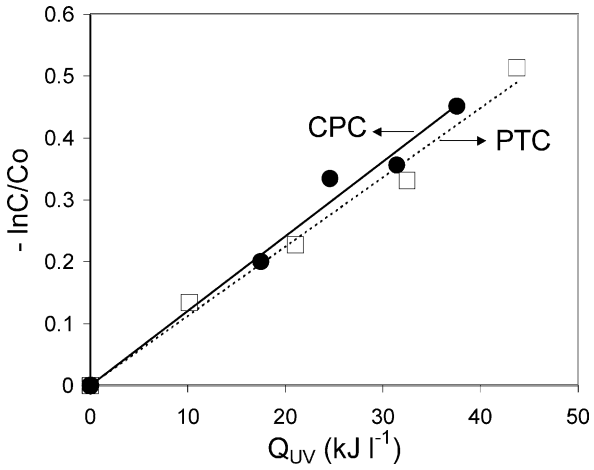

Fig. 3. Linear transform of kinetic curves of iron-photoassisted degradation of AMBI in a CPC and in a PTC. AMBI (1.0 mmol l^{-1}) and Fe^{3+} (1.0 mmol l^{-1}).

- Statistic analyses carried out at the PSA [23] revealed that the global radiation is higher than the direct radiation during all the year.

Other advantages of the CPC reactor have been previously reported [24,25]: low manufacturing, installation, and maintenance cost and the operational facilities. Considering these observations, the CPC appears as the best technology for a coupled solar-biological wastewater treatment system.

3.2. Comparison of different solar photocatalytic treatments using a CPC

A CPC, described in Section 2, was erected at EPFL. Various experiments were carried out in order to make an exploratory comparison of the efficiency of some solar photoassisted treatments on the degradation of AMBI.

Fig. 4 shows the evolution of AMBI concentration as a function of accumulated energy, when an aqueous solution of AMBI is exposed to light/TiO_2/O_2, light/TiO_2/H_2O_2, light/Fe^{3+}/O_2, and light/Fe^{3+}/H_2O_2 systems.

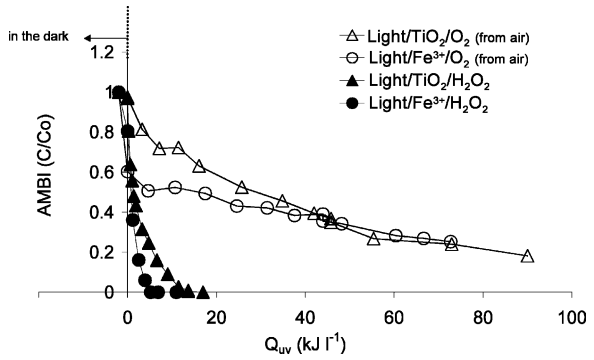

Fig. 4. Evolution of a DOC during AMBI degradation as a function of the accumulated solar energy. Study of some photocatalytic systems. AMBI (1.0 mmol l^{-1}), H_2O_2 (11 mmol l^{-1}), TiO_2 (1 g l^{-1}) and Fe^{3+} (1.0 mmol l^{-1}).

The results presented in Fig. 4 clearly demonstrate that both $h\nu$/Fe^{3+}/H_2O_2 and $h\nu$/TiO_2/H_2O_2 systems are effective, from the kinetic point of view, with an accumulated solar energy of 10 and 18 kJ l^{-1}, 100% of the initial AMBI concentration is eliminated from the solution using $h\nu$/Fe^{3+}/H_2O_2 and $h\nu$/TiO_2/H_2O_2 systems, respectively.

It was also observed that the performances of $h\nu$/Fe^{3+}/O_2 system are similar to those of the most common system studied, $h\nu$/TiO_2/O_2. The system $h\nu$/Fe^{3+}/O_2 appears as a new and interesting alternative for the treatment of pollutants in water.

Although the four oxidation systems are effective to the degradation of AMBI, the photo-Fenton process appears to be the most efficient. Moreover, its homogenous character provides with reasonable limitations good engineering conditions for coupling this system with a complementary biological treatment.

3.3. Optimization of Fe^{3+} and H_2O_2 concentration on the photo-Fenton degradation of AMBI using Response Surface Methodology

The effects of the two critical factors, hydrogen peroxide, and ferric ion concentration, on the photo-Fenton degradation of AMBI were simulated and evaluated, using the RSM [26]. This methodology has shown to be a valuable tool to model complex process such as the light-enhanced Fenton reaction and to achieve at minimal cost, optimal experimental parameters [27]. RSM is a collection of statistical and mathematical techniques useful for developing, improving, and optimizing processes performing a minimal number of well-chosen experiments [28]. It uses an empirical mathematical model (e.g. polynomial) to represent the response (y) in the experimental field which depends on the controllable inputs that are natural variables: $\xi_1, \xi_2, \ldots, \xi_k$.

$$y = f(\xi_1, \xi_2, \ldots, \xi_k) \tag{10}$$

Since, in this study the two natural variables: $\xi_1 = Fe^{3+}$ concentration (g l^{-1}); $\xi_2 = H_2O_2$ pumping rate (ml min^{-1}), are expressed in different units and have different limits of variation, their effects can only be compared by the RSM if they are coded.

To each natural variable ξ_i, there is a correspondent dimensionless coded variable x_i as defined in Eq. (11)

$$x_i = \frac{2(\xi_i - \xi_i^*)}{d_i} \tag{11}$$

where ξ_i is the actual value in original units, ξ_i^* the arithmetic mean of the high and low levels of i, and d_i the difference between the low and high levels of i.

In terms of the coded variables, the true response function (Eq. (10)) is now written as

$$y = f(x_1, x_2, \ldots, x_k) \tag{12}$$

Because the form of the true response function f is unknown, we approximate. So for, a Doehlert's uniform array was

Table 2
Experimental plan design and results obtained for the optimization of Fe^{3+} and H_2O_2 concentration in the photo-Fenton degradation of AMBI wastewater (5 mmol l^{-1}; DOC = 500 mg C l^{-1}) using a CPC reactor

Experiment number	Coded variables		Natural variables		Response
	Concentration of Fe^{3+}	H_2O_2	Concentration of Fe^{3+} (g l^{-1})	H_2O_2 pumping rate (ml min^{-1})	k_{app} (l kJ^{-1})
1	1.0000	0	0.2000	0.060	0.02
2	−1.0000	0	0	0.060	0.01
3	0.5000	0.8660	0.1500	0.112	0.02
4	−0.5000	−0.8660	0.0500	0.008	0.00
5	0.5000	−0.8660	0.1500	0.008	0.00
6	−0.5000	0.8660	0.0500	0.112	0.01
7	0	0	0.1000	0.060	0.01
8	0	0	0.1000	0.060	0.01
9	0	0	0.1000	0.060	0.01

employed allowing modelising the curve response surface. The associated response function (y) is represented by a quadratic polynomial model of the form:

$$y = b_0 + b_1x_1 + b_2x_2 + b_{12}x_1x_2 + b_{11}x_1^2 + b_{22}x_2^2 \quad (13)$$

where b_0, b_i, b_{ii}, and b_{ij} are the regression coefficients of the polynomial function. x_i and x_j, the concentration of Fe^{3+} and H_2O_2, are the coded variables and y is the apparent initial rate constant for the abatement of AMBI.

Table 2 presents the experimental matrix for seven experiments. The experimental points considering low and high levels for Fe^{3+} (0–0.2 g l^{-1}) and H_2O_2 (0.060–0.112 ml min^{-1}) are uniformly distributed in a spherical experimental domain. Experiment 7 was repeated twice more (8 and 9) in order to check the reproducibility.

The treatment of experimental responses, the mathematical resolution of the matrix, and the three-dimensional representation of the phenomenon were performed using the NEMROD Software [29].

The coefficients of the quadratic model in the polynomial expression (Eq. (13)) calculated by multiple regression analysis, are given in Eq. (14). These coefficients represent the weight of each variable, the quadratic effect, and the first-order interaction between the coded variables.

$$y = 0.012 + 0.007x_1 + 0.006x_2 + 0.005x_1x_2 + 0.002x_1^2 - 0.007x_2^2 \quad (14)$$

The polynomial equation permits to draw the contour plots and the three-dimensional representation of the phenomenon (Fig. 5).

Fig. 5 shows that, for all iron concentrations, the H_2O_2 concentration has an optimum value in which the k_{app} reaches a maximum. For high H_2O_2 concentrations the AMBI degradation decays. The effect is more clear when the iron concentration is low.

The detrimental effect of higher H_2O_2 concentrations is probably due to both auto-decomposition of H_2O_2 into oxygen and water (15), and the recombination of $^{\bullet}OH$ (16) as follows:

$$2H_2O_2 \rightarrow 2H_2O + O_2 \quad (15)$$

$$^{\bullet}OH + H_2O_2 \rightarrow {}^{\bullet}O_2H + H_2O \quad (16)$$

Maximum degradation rate was predicted in the region of 0.15–0.2 g l^{-1} of Fe^{3+} and 0.06–0.12 ml l^{-1} of H_2O_2. Taking into account the initial AMBI concentration, it is observed that optimal ratio of AMBI/Fe^{3+}/H_2O_2 of 1/0.1/10 provides optimal performances for AMBI degradation.

3.4. Chemical and biological characteristics of photo-treated solutions

Considering that the basic objective of this investigation was not to achieve the complete photo-mineralization, but to reach a biocompatible solution that can be conducted

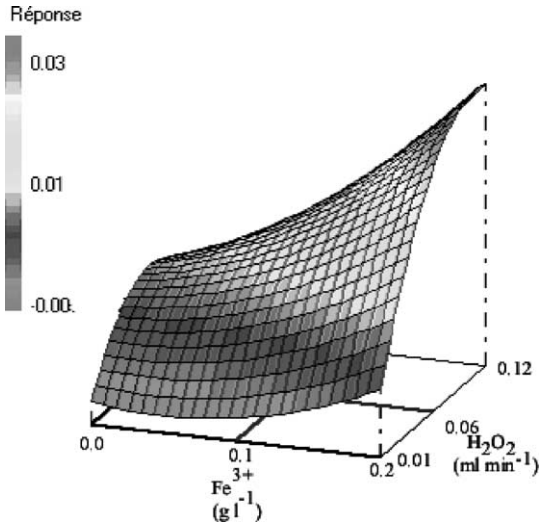

Fig. 5. Optimization of Fe^{3+} and H_2O_2 concentration for solar photo-Fenton degradation of AMBI using Surface Response Methodology. Three-dimensional representation of the response surface for the apparent initial rate constant (k_{app}).

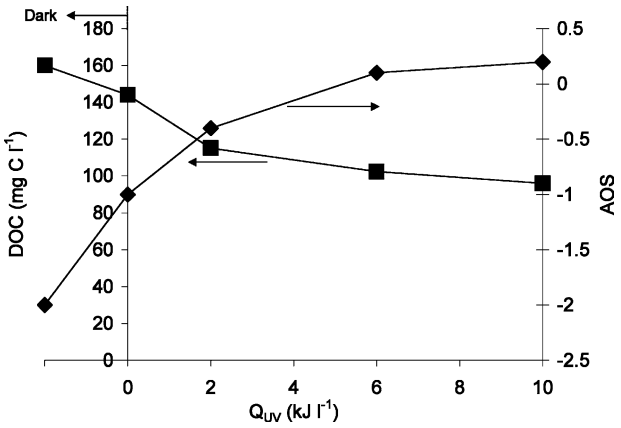

Fig. 6. AMBI concentration and AOS evolution as a function of accumulated energy for the degradation of 60 l of real AMBI wastewater. AMBI (1 mmol l^{-1}), Fe^{3+} (0.1 mmol l^{-1}) and H_2O_2 (10 mmol l^{-1}).

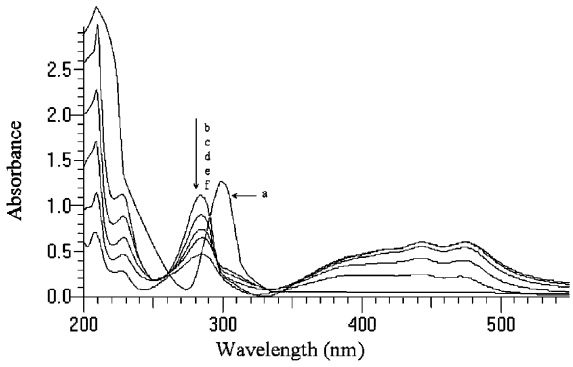

Fig. 7. UV-Vis spectra evolution of AMBI solutions during a solar photo-Fenton degradation experiment in a CPC. (a) Initial AMBI, (b) AMBI + Fe^{3+}, (c) solution after Q_{UV} = 2 kJ l^{-1}, (d) solution after Q_{UV} = 4 kJ l^{-1}, (e) solution after Q_{UV} = 6 kJ l^{-1}, and (f) solution after Q_{UV} = 10 kJ l^{-1}.

towards a biological process, it was necessary to assess the chemical and biological characteristics of the residual DOC contained in the photo-treated solutions.

Several experiments were carried out in order to obtain information concerning the evolution of the biorecalcitrant compound concentration and the AOS, with the aim to define the moment when photo-treatment can be stopped to lead the solution to the biological reactor.

Fig. 6 shows the profile of AMBI concentration and the AOS as a function of accumulated amount of energy per unit of volume (kJ l^{-1}). During the first part (dark conditions) almost 10% of the initial DOC concentration is removed. This can be attributed to the complexation of AMBI by Fe(III) as well as the dark Fenton reactions. Upon solar illumination (photo-Fenton reaction) the degradation rate is clearly improved and almost 40% of the initial AMBI is removed when 10 kJ l^{-1} are accumulated in the CPC.

The AOS, a gross parameter useful to estimate the oxidation degree of mixed solutions and gives indirect information on its probability to biodegrade, was calculated using Eq. (17) [2]:

$$\mathrm{AOS} = \frac{4(\mathrm{TOC} - \mathrm{COD})}{\mathrm{TOC}} \tag{17}$$

where TOC and COD are expressed in mmol C l^{-1} and mmol O_2 l^{-1}, respectively. AOS takes values between +4 for CO_2, the most oxidized state of C, and −4 for CH_4, the most reduced state of C. From Fig. 6 it is observed that the AOS value increased as a function of the accumulated energy and attained almost a plateau after approximately 8 kJ l^{-1}. This results suggest that more oxidized intermediates are formed in solution and after 8 kJ l^{-1}, the chemical nature of most of them does not vary anymore even if the photo-treatment is prolonged. Formation of very oxidized intermediates is an indirect indication of the ability of the solar pretreatment to improve the biodegradability of real AMBI wastewater.

Moreover, as indicated in previous works [12,13], according to different biodegradability test using Zahn–Wellens procedures [30] as well as on a FBR, the AMBI solution becomes biocompatible after the complete elimination of the initial biorecalcitrant compound (AMBI). This phenomenon is accompanied by the concomitant elimination of 45% of the initial DOC, and the AOS reaches a value around 0.2.

UV-Vis spectroscopy analyses were performed within the photo-Fenton degradation experiment and the results are presented in Fig. 7.

The spectra of AMBI have a maximum at 300 nm. The spectrum of the mixture (AMBI + Fe^{3+}) has a maximum at 284 and 475 nm. This mixture leads presumably to the formation of a complex, which have significant absorption in the visible region. The solar irradiation leads to a diminution of the long-wavelength absorption as shown in spectra (b)–(f).

According to the previous observations, it is possible to represent the AMBI degradation by the following simplified schema Fig. 8. A reduction–oxidation cycle of Fe(III)–Fe(II) and the photolysis of Fe(III) aqueous complexes generating $^{\bullet}$OH radicals and the formation of a photoactive complexes [AMBI···Fe(III)] seems to be the possible ways for the photo-Fenton degradation of AMBI.

3.5. Performances of the coupled solar-biological flow system

The coupled reactor shown in Fig. 1 was operated in semi-continuous mode. The photochemical step treats the AMBI solution in batch cycles providing photo-treated water to the biological reactor. This operation mode was chosen since it gave better results, at lab scale compared to the continuous mode [9]. The main parameters affecting the performance of the whole system operating in continuous mode are related to: (i) the pollutant concentration that can be treated, (ii) the antiphysiological effect of H_2O_2 remained in the photo-treated solution, and (iii) the non-continuous solar-UV power while the circulation flow rate of water solution is constant.

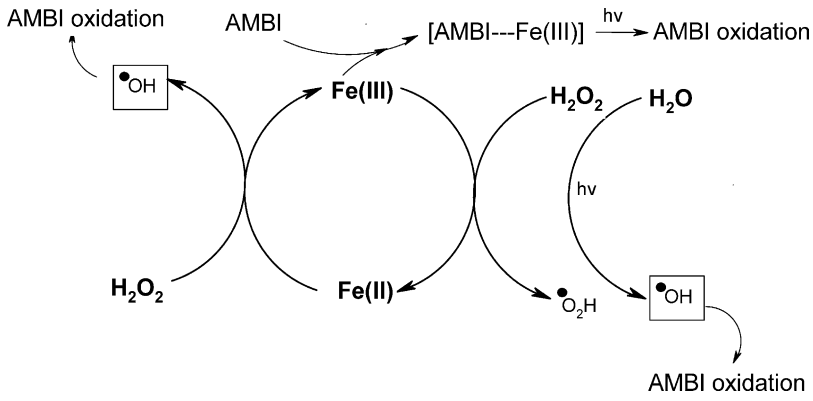

Fig. 8. Simplified schematic representation of photo-Fenton degradation of AMBI.

The coupled reactor was operated using photo-Fenton pretreatment and the results are presented in Fig. 9. From this figure, it is observed that with an accumulated solar energy of 10 kJ l^{-1}, 100% of the initial biorecalcitrant compound (AMBI) was degraded.

The pretreated solution flowed to the biological reactor, where the complete mineralization was achieved in 20 h, indicating that the photo-pretreatment is able to produce a biocompatible solution.

Considering the efficiency of the solar photo-Fenton pretreatment for AMBI degradation, some experiments were carried in order to test if it is a practical application for the degradation of real wastewaters more concentrated with AMBI.

The input organic load was incremented in the rage of 100–800 mg C l^{-1} in order to find out the maximal concentration of AMBI that can be treated by the coupled reactor. Optimal AMBI/Fe^{3+}/H_2O_2 ratio was utilized in each experiment. The AMBI wastewater is photo-treated in semicontinuous mode, same as in the previous experiments, and when 100% of AMBI degradation is attained, the pretreated solution is then lead into the biological reactor.

Fig. 10 shows the percentage of DOC removed in the solar, the biological and the whole coupled reactor as a function of the initial DOC of the solution.

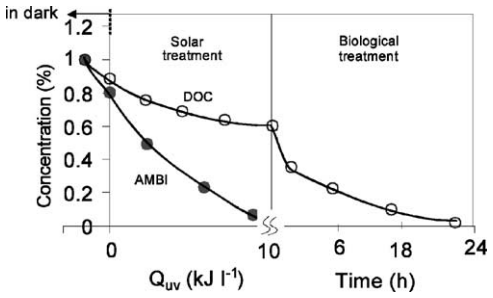

Fig. 9. Evolution of AMBI and DOC concentration during the solar photo-Fenton and biological treatment. AMBI (1.0 mmol l^{-1}), Fe^{3+} (0.1 mmol l^{-1}), and H_2O_2 (10 mmol l^{-1}).

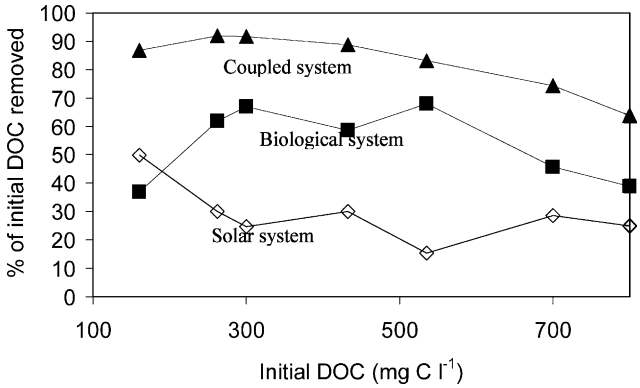

Fig. 10. DOC removal by solar, biological and coupled treatment as a function of the initial organic load in the coupled reactor.

In Fig. 10, it is observed that the solar system is able to remove 50% of the initial DOC with an initial load of 160 mg C l^{-1}. However, this efficiency is considerably diminished when the initial organic load increases form 160 to 300 mg C l^{-1}, reaching 30% of efficiency for the same energy accumulated. The DOC removal efficiency of the biological reactor is 60% until 500 mg C l^{-1}, but an important diminution is observed for higher concentrations, probably due to inhibition of the micro-organisms. Nevertheless, a whole performance of 80–90% is reached in the range of 300–500 mg C l^{-1}, indicating the plausibility of the coupled approach at pilot scale in the context of the treatment a real industrial wastewater.

4. Conclusions

In this paper an overview of recent works (1998–2002) coupling photoassisted AOPs and biological process wastewater treatment was performed. This overview confirms the beneficial effects of such two-steps treatment at lab scale and the lack of studies carried at field scale with the same approach.

An innovative coupled solar-biological system at field pilot scale was designed, builds, and tested on the degradation of a biorecalcitrant model compound: AMBI. The strategy follows to develop this system has shown that:

(i) the CPC was the most appropriate to be coupled with a biological reactor;
(ii) among the tested AOPs for the degradation of the AMBI, the photo-Fenton process is the most efficient;
(iii) using the Surface Response Methodology to optimize the Fe^{3+} and H_2O_2 concentration in the photo-Fenton system, the AMBI/Fe^{3+}/H_2O_2 ratio of 1/0.1/10 provides the optimal performance;
(iv) the photo-Fenton pretreatment is able to completely remove the pollutant (AMBI), as well as to improve the AOS of the solution, generating a biocompatible effluent.

Using an immobilized-cell aerobic reactor in the biological part of the system, the evaluation of the so coupled solar-biological flow system demonstrated that, when operating in semicontinuous mode, it is able to reach a whole performance of 80–90% in the range of 300–500 mg C l^{-1}. This result indicates the plausibility of using the coupled approach at pilot scale to treat real industrial wastewaters.

Acknowledgements

This work was supported by the OFES contract No. 01.0433 within the CADOX research program EUK1-CTIC1-CT-2002-00122 of the European Community. We thank Dr. Sixto Malato of the Plataforma Solar de Almeria (PSA) for his help throughout the work. We are pleased to thank “DLK Technologies SA” for the doctoral grant of V. Sarria. The skilful technical assistance of J.P. Kradolfer is duly appreciated. We wish to express our gratitude to the “*Project environment EPFL-UNIVALLE*.”

References

[1] D.F. Ollis, H.A. Ekabi, Photocatalytic purification and treatment of water and air, in: EDS, Elsevier, Amsterdam, 1993.
[2] J.P. Scott, D.F. Ollis, Environ. Prog. 14 (1995) 88.
[3] J.P. Scott, D.F. Ollis, J. Adv. Oxid. Technol. 2 (1997) 374.
[4] C.D. Adams, J.J. Kuzhikannil, Water Res. 34 (2000) 668.
[5] F.J. Benitez, J.L. Acero, T. Gonzalez, J. Garcia, Ind. Eng. Chem. Res. 40 (2001) 3144.
[6] T.F. Hess, T.A. Lewis, R.L. Crawford, S. Katamneni, J.H. Wells, R.J. Watts, Water Res. 32 (1998) 1481.
[7] S. Ledakowicz, M. Solecka, R. Zylla, J. Biotechnol. 89 (2001) 175.
[8] S. Parra, V. Sarria, S. Malato, P. Peringer, C. Pulgarin, Appl. Catal. B 27 (2000) 153.
[9] C. Pulgarin, M. Invernizzi, S. Parra, V. Sarria, R. Polania, P. Peringer, Catal. Today 54 (1999) 341.
[10] M. Rodriguez, V. Sarria, S. Esplugas, C. Pulgarin, J. Photochem. Photobiol. A 151 (2002) 129.
[11] J. Reyes, M. Dezotti, E. Esposito, J. Villasenor, H. Mansilla, N. Durnan, Appl. Catal. B 15 (1998) 211.
[12] V. Sarria, S. Parra, M. Invernizzi, P. Péringer, C. Pulgarin, Water Sci. Technol. 44 (2001) 93.
[13] V. Sarria, M. Deront, P. Peringer, C. Pulgarin, Appl. Catal. B 40 (2003) 231.
[14] M.C. Yeber, J. Freer, M. Martinez, H.D. Mansilla, Chemosphere 41 (2000) 1257.
[15] S. Parra, S. Malato, C. Pulgarin, Appl. Catal. B 36 (2002) 131.
[16] Y.F. Sun, J.J. Pignatello, Environ. Sci. Technol. 27 (1993) 304.
[17] G. Mailhot, A. Asif, M. Bolte, Chemosphere 41 (2000) 363.
[18] V. Sarria, S. Parra, N. Adler, P. Péringer, C. Pulgarin, Catal. Today 76 (2002) 301.
[19] M. Martienssen, Water Res. 34 (2000) 3917.
[20] D.F. Ollis, Water Sci. Technol. 44 (2001) 117.
[21] S. Malato, J. Caceres, A. Agüera, M. Mezcua, D. Hernando, J. Vial, A.R. Fernández-Alba, Environ. Sci. Technol. 35 (2001) 4359.
[22] C. Minero, E. Pelizzetti, S. Malato, J. Blanco, Chemosphere 26 (1993) 2103.
[23] J. Blanco, S. Malato, Tecnología de Fotocatálisis Solar: Utilización de la Radiación Solar Para el Tratamiento de Contaminantes Industriales, CIEMAT, Almeria, 1996, p. 102.
[24] S. Malato, J. Blanco, C. Richter, D. Curco, J. Gimenez, Water Sci. Technol. 35 (1997) 157.
[25] S. Parra, S. Malato, J. Blanco, P. Péringer, C. Pulgarin, Water Sci. Technol. 44 (2001) 219.
[26] A.I. Khuri, J.A. Cornell, Response Surfaces, Designs and Analyses, Dekker, ASQC Quality Press, New York, 1987.
[27] E. Oliveros, O. Legrini, M. Hohl, T. Muller, A.M. Braun, Water Sci. Technol. 35 (1997) 223.
[28] R.H. Myers, D.C. Montgomery, Response Surface Methodology: Process and Product Optimization Using Designed Experiments. Wiley Series in Probability and Statistics, Wiley, New York.
[29] D. Mathieu, J. Nony, R. Phan-Tan-Luu, NEMROD, L.P.R.A.I., Université d’Aix-Marseille, France, 2000.
[30] OECD, Guidelines for Testing of Chemicals, Vol. 2, Test 302B, 1996.